Influence of Phase Microstructure on the Mechanical Properties of Ternary Phase Polypropylene Composites

P. R. HORNSBY,[1] K. PREMPHET[2]

[1] Department of Materials Engineering, Brunel University, Uxbridge, Middlesex UB8 3PH, United Kingdom

[2] Department of Chemistry, Mahidol University, Rama VI Road, Bangkok 10400, Thailand

Received 12 January 1998; accepted 25 March 1998

ABSTRACT: The mechanical properties and phase microstructure of ternary phase polypropylene composites have been investigated using combinations of rigid glass beads and ethylene/propylene rubber (EPR) modifiers. Particular consideration has been given to the relative interaction between these components and their dispersion within the composite. In this regard, EPR and untreated glass beads existed as independent phases, whereas EPR functionalized with maleic anhydride showed a tendency to encapsulate the inorganic phase. As a consequence, marked differences in mechanical properties, in particular toughness, were exhibited by these systems, manifested by changes in failure mechanism. Structure in these composites was explored by Fourier transform infrared spectroscopy, dynamic mechanical analysis, and scanning electron microscopy. © 1998 John Wiley & Sons, Inc. J Appl Polym Sci 70: 587–597, 1998

Key words: composites; fillers; rubber microstructure

INTRODUCTION

Polypropylene (PP), although, extensively used in many fields of application, is limited by its low temperature impact strength. One of the most widely used methods to overcome this drawback is by blending with other polymers, especially elastomers. Although rubber modification of PP increases its low temperature impact strength, stiffness is lowered. To compensate for this effect, filler can also be added to the blend, creating a ternary phase composite.[1–11] In these materials containing both elastomer and rigid filler, two extremes in phase structure may occur, where either elastomer and filler particles are dispersed separately in the PP matrix[6,12] or the rubber encapsulates filler particles, resulting in a low modulus interlayer between matrix and filler.[13,14] The relative extent to which these structures develop depends on several factors, especially the surface characteristics and mutual wettability of fillers and polymer, blend preparation techniques (including the sequence in which the components are introduced into the blend), and the relative viscosity of the polymer and elastomeric phases.

In the present study, ternary phase PP composites, containing ethylene/PP rubber (EPR) and glass beads, were investigated. The aim of this work was to explore relationships between the microstructure and mechanical properties of these materials. In this regard, particular attention has also been given to the influence of surface-treated filler [silane-coated glass beads (coatG)] and functionalized rubber (maleic anhydride-modified EPR).

Correspondence to: P. R. Hornsby.

Journal of Applied Polymer Science, Vol. 70, 587–597 (1998)
 CCC 0021-8995/98/030587-11

EXPERIMENTAL

Materials

PP homopolymer Novolen 1100HX [melt flow rate (MFR) = 1.8 g/10 min] supplied by BASF, was used as the matrix polymer. There were two grades of EPR used: Exxelor PE808 and Exxelor VA1803, both supplied by Exxon Chemical Co. The former is a medium viscosity semicrystalline polymer (MFR = 5 g/10 min), whereas the latter is a low-viscosity amorphous maleic anhydride-grafted EPR (MFR = 22 g/10 min), with a maleic anhydride content of 0.7% by weight. Glass beads were used in the untreated form (5000 CP00) and surface-modified with silane coupling agent (5000 CP03). Both variants were supplied by Croxton & Garry Ltd., with particle diameters in the range of 4.0–7.0 μm.

Compounding

Blends of various compositions were prepared by melt-mixing in a BTS 40 intermeshing corotating twin-screw extruder (Betol Machinery Ltd.) using a barrel temperature profile of 185–200°C (from feed zone to die). Samples were produced at a screw speed of 170 rpm, giving a throughput rate of $\sim$ 20 kg h^{-1}.

Specimen Preparation

Test specimens for morphological and mechanical testing were prepared by compression molding, using a horizontal flash-type mold with dimensions of 23 $\times$ 23 $\times$ 0.2 cm. The molding procedure involved heating the materials at 200°C for 8 min without applied pressure and then subsequently for a further 5 min under pressure. The mold was then rapidly cooled to room temperature within a period of 3 min. By this means, uniform and void-free specimens were produced.

Mechanical Testing

Tensile dumbbell specimens were cut from the 2-mm-thick-molded sheet and tested using an Instron model 4206 tensile testing machine using a crosshead speed of 50 mm min^{-1}. Test specimens for instrumental impact testing were in the form of 70 $\times$ 70 $\times$ 2-mm-thick-molded plaques clamped on a steel ring having an internal diameter of 40 mm. A 5 kg flat-headed 10 mm diameter tup was dropped onto the specimens from a height of 46 cm, generating an impact velocity of 3 m s^{-1}. All mechanical testing was undertaken at 23°C.

A Rheometrics dynamic mechanical analyzer (RSAII) was used for measuring the mechanical properties of the composites over a temperature range of -100 to 100°C. Testing was conducted in three-point bending mode using a frequency of 6.28 rad s^{-1} (1 Hz).

Structural Analysis

Representative samples were analyzed in a Perkin–Elmer DSC-7 differential scanning calorimeter using a thermal cycling procedure.

The instrument was first calibrated using indium as a reference material. Sample mass was maintained at 7 $\pm$ 1 mg, and all materials were analyzed at the same scan rate. Using multiple specimens, the technique was found to give reproducible melting and crystallization temperatures to an accuracy of $\pm$0.2°C. Samples were first heated from 30° to 210°C at a rate of 10°C min^{-1}. The temperature was then maintained at 210°C for 10 min before cooling to 30°C at the same rate, then reheating to 210°C, again at 10°C min^{-1}. Melting and crystallization temperatures were recorded. The percentage crystallinity was calculated from the heat of fusion using a $\Delta H°$ value of 189 J g^{-1} for isotactic polypropylene (iPP).[15]

Films of $\sim$ 15 μm thick were prepared by hot-pressing, and analyzed in a Nicolet 710 Fourier transform infrared spectrometer, equipped with a data processing computer.

Phase structures of the composites were examined by scanning electron microscopy on etched fracture surfaces. These were exposed to hot heptane vapor for 3 min to remove the EPR particles from the PP matrix and thus improve contrast between the phases. All samples were sputter-coated with gold-palladium alloy before viewing under Cambridge S-250 Stereoscan scanning electron microscope.

RESULTS AND DISCUSSION

Phase Morphology

Figure 1(a) shows the microstructure of the polypropylene/ethylene–propylene rubber/glass (PP/EPR/G) composite, where there is no evidence of EPR encapsulation around the inorganic filler. Glass beads are seen to be well dispersed without

particle agglomeration. A contrasting morphology is shown in Figure 1(b) for the PP/maleic anhydride modified rubber/G composite, where there is evidence of MaR encapsulation around the rigid filler particles. The effect of using silane-coated glass beads is apparent in Figure 1(c) for the PP/EPR/coatG composite, where the phases are separately dispersed. However, some glass bead particles were found to be partially wetted by EPR, as seen in Figure 1(d. Here, the small dark circular holes ($\sim$ 1 μm diameter) are imprints of EPR particles, whereas large hemispherical dark areas ($\sim$ 5–7 μm diameter) are formed as glass bead particles are pulled out during fracture.

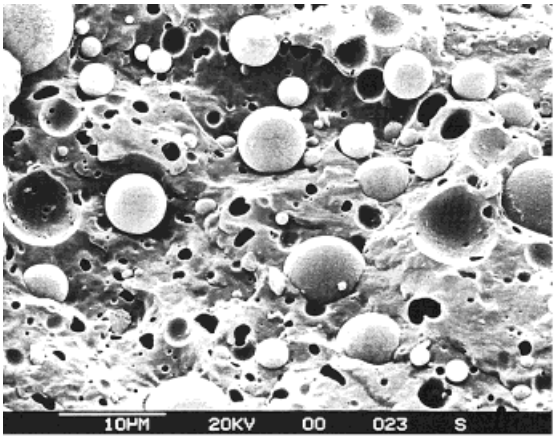

(a)

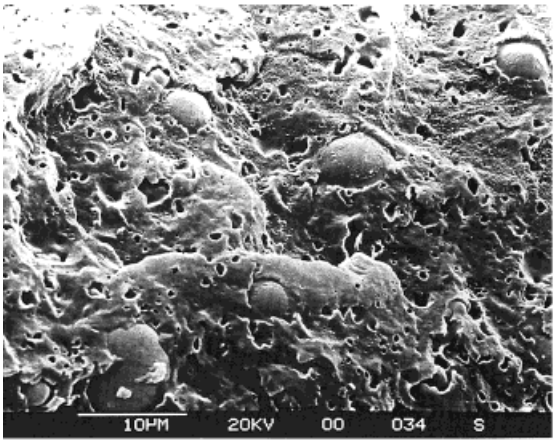

(b)

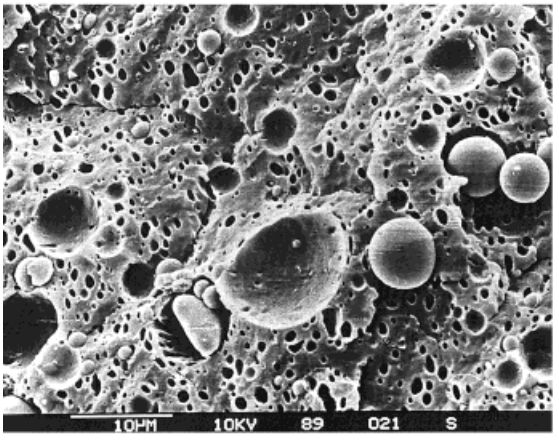

(c)

Figure 1 Microstructure of ternary phase composites after cryogenic fracture and etching. (a) PP/EPR/G; (b) PP/MaR/G; (c) and (d) PP/EPR/coatG.

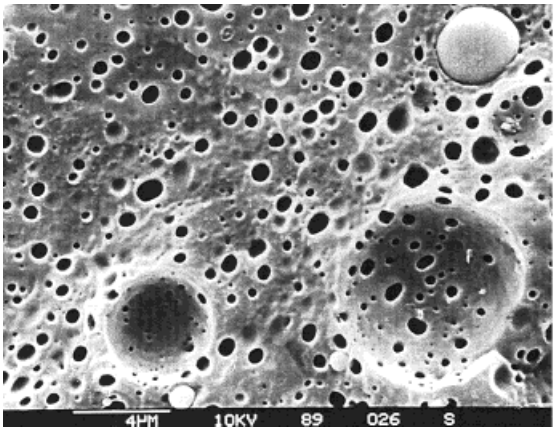

(d)

Figure 1 (*Continued*)

The extent of filler wet-out by a liquid phase depends on the nature of the solid surface, including its surface energy and roughness, the viscosity and amount of liquid available, and the contact angle between liquid and solid. Critical surface tension values for PP and EPR are reported to be $\sim$ 29–32 mJ m^{-2} (refs. 16 and 17) and 28 mJ m^{-2} (ref. 18), respectively, reflecting similarities in their chemical composition. Although these data infer that both PP and EPR would wet glass bead particles to a similar degree, due to the lower viscosity and higher concentration of PP in the compositions, glass bead particles were more favorably coated by PP than by EPR in the PP/EPR/G composite, resulting in separate dispersion of the EPR and glass bead phases.

Conversely, in the PP/MaR/G composites, glass bead particles were preferentially wetted by MaR, giving rise to an encapsulated structure. This observation can be explained by the higher surface tension of MaR relative to PP,[3] due to the functionalization of EPR with maleic anhydride. However, owing to the high viscosity of this melt and the dewetting that inevitably occurs during high shear mixing, complete encapsulation is not achieved.

In compositions where the glass beads had been pretreated with silane coupling agent (PP/

EPR/coatG), a separate dispersion structure was again observed. Literature reports for commonly used silane coupling agents give critical surface tensions of coated glass ~ 31–36 mJ m^{-2} (refs. 19 and 20). Hence, after surface treatment, the lower surface energy of the filler makes it more amenable to wet-out by polymer melt, although as with the PP/EPR/G composite, interaction with the PP-rich phase dominates.

Figure 2(a) shows a cryogenic (nonetched) fracture surface of the unmodified PP/EPR/G composite, demonstrating failure at the weak interface between PP and glass beads. Furthermore, it would appear that some of the EPR particles were elongated and detached from the PP matrix, leaving small spherical holes on the fracture surface. Comparing Figure 2(a,b) reveals distinctly different fracture morphologies. In the PP/MaR/G system, adhesion between the PP matrix and glass beads, and also between the PP matrix and EPR, is greater than the inherent strength of the matrix, causing crack propagation through the PP phase and resulting in cohesive failure. This is manifested by an absence of glass particles seen on the fracture surface. However, in the PP/EPR/coatG composite, even though the glass beads had been treated with silane coupling agent, no significant improvement in adhesion to PP was observed [Fig. 2(c)].

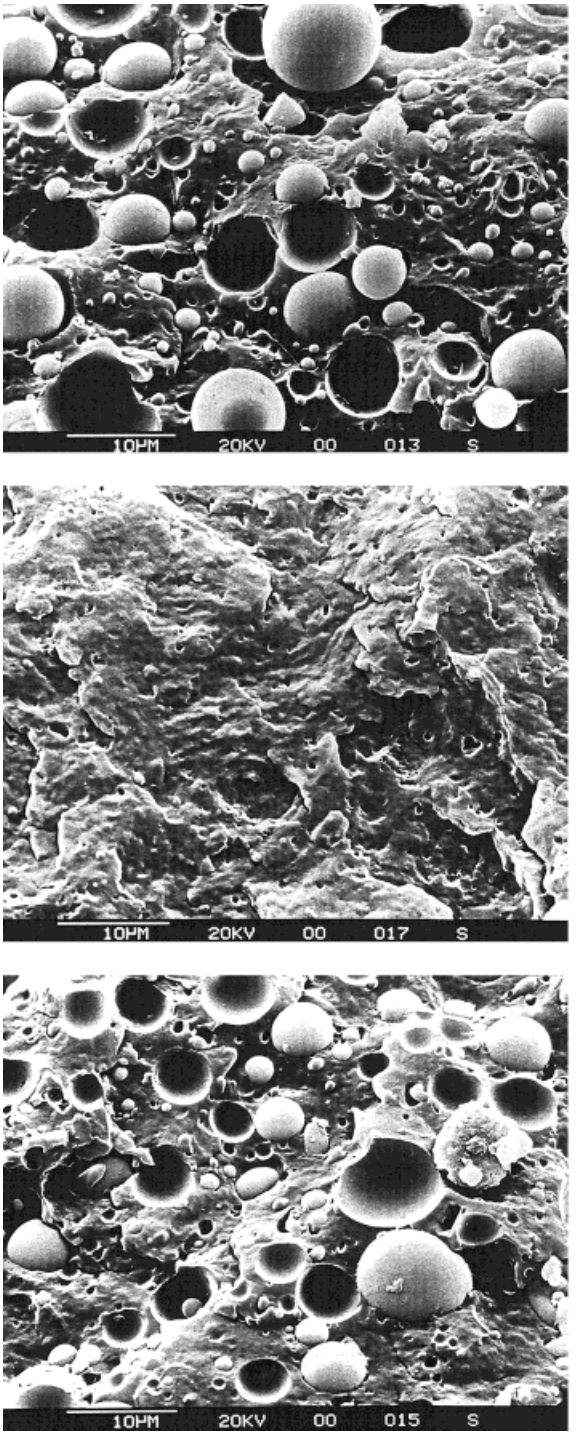

(a) (b) (c)

Figure 2 Microstructure of ternary composites after cryogenic fracture without etching. (a) PP/EPR/G; (b) PP/MaR/G; (c) PP/EPR/coatG.

Dynamic Mechanical Analysis

Temperature dependencies of tan δ at 1 Hz are shown for various composites in Figure 3(a). In both PP/EPR/G and PP/MaR/G composites, two tan δ peaks were observed, corresponding to the glass transition temperatures (T_g) for PP and incorporated rubber. The location and intensity of T_g peaks for PP in both composites were the same at 7°C. A T_g value for EPR in the PP/EPR/G composite was observed at −43°C, which is similar to that observed in the binary PP/EPR blend [Fig. 3(b)], indicating that glass beads had no influence on the mobility of the rubber chains. This reflects a lack of association between EPR and glass beads in this composition.

However, it is significant that the T_g peak for MaR shifted from −61°C (in the binary blend) to −56°C (in the ternary blend). This suggests that, in this system, the incorporation of glass beads causes immobilization of rubber chains. Also, the dynamic mechanical analyzer spectrum for PP/MaR/G showed a much larger and broader rubber glass transition than in the corresponding PP/EPR/G composite. This is attributed to the encapsulation of rubber around the filler particles when

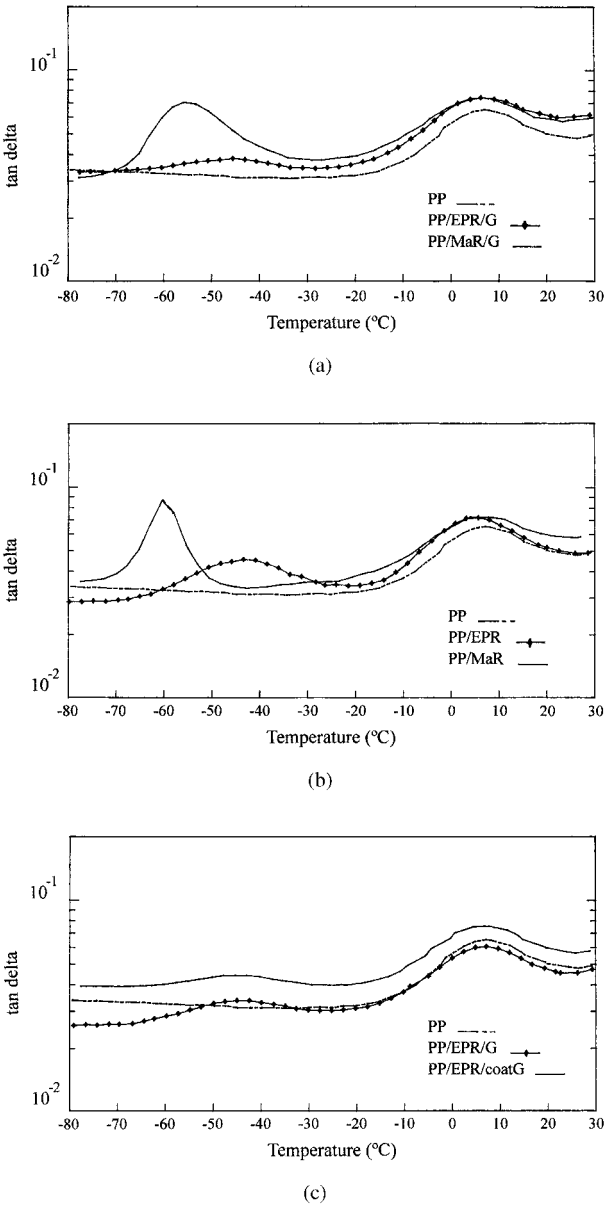

Figure 3 Dynamic mechanical analysis of PP binary and ternary phase composites at 1 Hz. (a) Temperature dependency of tan δ for PP, PP/EPR/G (70/15/15), and PP/MaR/G (70/15/15) composites. (b) Temperature dependency of tan δ for PP, PP/EPR (70/30), and PP/MaR (70/30) blends. (c) Temperature dependency of tan δ for PP, PP/EPR/G (70/15/15), and PP/EPR/coatG (70/15/15) composites.

MaR is present, because the size of the tan δ peak for the rubber phase is influenced not only by the amount of rubber, but also by particulate inclusions within the rubbery phase.

There is essentially no difference between the dynamic mechanical spectra for composites containing untreated and surface-coated glass beads [Fig. 3(c)]. Furthermore, the use of coated glass beads did not appreciably affect the T_g of either PP or rubber, confirming that filler and rubber are independently dispersed in the PP matrix.

Differential Scanning Calorimetry (DSC)

Table I summarizes the DSC results for unmodified PP, binary blends of PP containing either rubbery particles or glass beads, together with their corresponding ternary phase compositions. In the binary blends, the addition of 30 vol % of EPR caused a reduction in the T_c, $T_{c\text{onset}}$, and T_m values for PP. The percentage crystallinity observed in the PP/EPR blend was found to be lower than that for unmodified PP. However, this reduction is entirely attributed to the substitution of 30 wt % of PP by EPR, which did not crystallize under the DSC testing conditions used.

Maleic-anhydride-modified EPR had no effect on the $T_{c\text{onset}}$ and T_c values for PP. However, values for T_1 and T_2 (defined in Table I) were lower than for unmodified PP. It may be inferred from these results that MaR increases the rate of crystallization leading to the development of smaller spherulites, which because of their decreased heat capacity shifted the melting temperature of the blend to a lower temperature.

In the PP/G blends, an opposite effect was observed. The incorporation of 30 vol % of glass beads to PP led to an increase in $T_{c\text{onset}}$ and T_c for PP, with a marked reduction in the degree of undercooling and a smaller difference between T_c and $T_{c\text{onset}}$. Again, the percentage crystallinity observed in the PP/G composite was lower than that for unmodified PP, which can be accounted for by the substitution of PP by 30 vol % (54 wt %) of glass beads.

In the ternary phase, PP/EPR/G composite where both EPR and G were present, polymer crystallization and melting temperatures were intermediate between those for PP/EPR and PP/G composites, indicating that both EPR and G had an independent effect on the crystallization and melting behavior of PP, since they existed as discrete phases in the composite. Contrary results were found for the PP/MaR/G composite, however. From the DSC results for the binary PP/MaR blend, it was apparent that MaR has no effect on the $T_{c\text{onset}}$ of PP. Thus, in the corresponding ternary phase composite, it was expected that only glass beads would influence the

Table I Thermal Properties of Binary and Ternary Phase PP Composites

Sample	Composition (% by vol)	T_{conset} (°C)	T_c (°C)	T_m (°C)	Crystallinity (%)	T_1 (°C)	T_2 (°C)
PP	100	114.6	109.5	164.3	49.0	5.1	54.8
PP/EPR		113.4	108.4	162.5	34.4	5.0	54.1
PP/MaR	70/30	114.5	109.9	160.5	35.4	4.6	50.6
PP/G		120.9	117.1	162.7	24.7	3.8	45.6
PP/EPR/G		116.7	111.8	162.3	26.2	4.9	50.5
PP/MaR/G	70/15/15	114.6	110.2	162.2	27.5	4.4	52.0
PP/EPR/coatG		119.5	114.8	162.6	26.3	4.7	47.8

T_{conset}, temperature of onset of crystallization; T_c, crystallization temperature; ΔH_c, heat of crystallization; T_m, melting temperature; ΔH_m, heat of fusion; T_1, $T_{conset} - T_c$; T_2, $T_m - T_c$.

T_{conset} of PP, and hence yield results similar to those observed in the PP/G composite, without rubber present. However, the observed T_{conset} value in the PP/MaR/G composite was only 114.6°C, demonstrating a marked suppression in the influence of glass beads on the T_{conset} of PP due to their encapsulation by functionalized rubber. In the PP/EPR/coatG composite, the glass beads had a strong nucleating effect on the crystallization behavior of PP, confirming the earlier finding that the structure in this composite comprised separately dispersed phases.

Fourier Transform Infrared (FTIR)

FTIR spectroscopy was used to investigate the chemical nature of the glass–polymer interface, particularly with regard to the PP/MaR/G composite. The infrared spectra of maleic anhydride functionalized EPR (MaR) is given in Figure 4 over a frequency range from 1800 to 1300 cm^{-1}. The large peaks at 1461 and 1375 cm^{-1} are attributed to C—H stretching vibrations in the methylene and methyl groups present in the rubber. The small absorption at 1713 cm^{-1} arises from the acid peak of the maleic anhydride modification. In general, the anhydride modification may exist in the anhydride or acid forms,[21] which are reversible by the addition or removal of water. The acid peak normally exists at $\sim$ 1714 cm^{-1}, whereas the anhydride absorptions appear as two peaks, one at 1864 cm^{-1} and a larger one at 1789 cm^{-1}.

Figure 5 shows infrared spectra for the MaR and MaR/G compositions. When glass beads are present, the anhydride peak of MaR at 1714 cm^{-1} disappears, with a new peak visible at 1571 cm^{-1}. This was also seen at 1565 cm^{-1} in the PP/MaR/G blend. These absorptions arise from asymmetrical stretching of the carboxylate ion (CO_2^-) formed due to reaction between MaR and glass beads. A similar observation was reported by Scott and colleagues,[22] in which a new peak appeared at 1568 cm^{-1} due to the CO_2^- salt produced from the reaction of maleic anhydride-modified ethylene–propylene terpolymer with γ-aminopropyltriethoxysilane. In this instance, a cyclic imide product was identified from the reaction.

The infrared spectra for EPR/coatG and PP/EPR/coatG composites are illustrated in Figure 6. No absorption band was seen in the range of 1800 to 1500 cm^{-1}, and the spectra for composites containing silane-coated glass particles were found to be very similar to that of PP/EPR/G, without glass treatment. Hence, the spectroscopic evidence suggests that the silane-coated glass beads did not

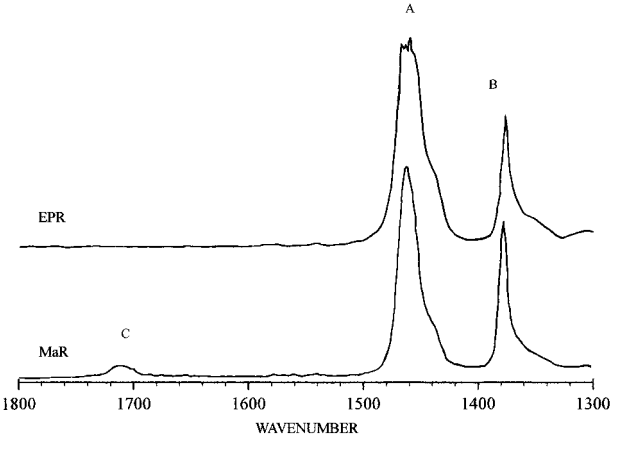

Figure 4 FTIR spectra of EPR and MaR. (A) C—H stretch (CH_2 group); (B) C—H stretch (CH_3 group); (C) C═O stretch maleic acid modification.

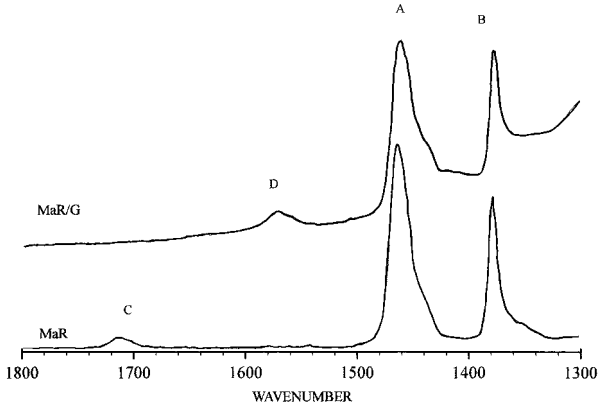

Figure 5 FTIR spectra of MaR/G and MaR. (A) C—H stretch (CH_2 group); (B) C—H stretch (CH_3 group); (C) C═O stretch maleic acid modification; (D) C═O stretch of carboxylate anion.

react with polymer. Bonding of silane coupling agents to the polymer generally occurs through interdiffusion of oligomeric siloxanes at the interface, with possible crosslinking to form an interpenetrating polymer network in this region.[23]

Mechanical Properties

The influence of EPR, MaR, and uncoated glass beads on the composite modulus is shown in Figure 7. It is evident that incorporation of 30 vol % EPR markedly reduces stiffness, whereas modulus of the ternary phase PP/EPR/G composite is noticeably increased with glass bead content. No significant difference was seen between EPR and MaR on Young's modulus of the binary (70/30) blends; however, in ternary phase composites, modulus was found to depend on the microstructure developed. In particular, the presence of functionalized rubber (i.e., PP/MaR/G) gave significantly lower modulus values than was the case when unfunctionalized EPR was present. It was demonstrated earlier that the interaction between MaR and glass beads occurs through the formation of carboxylate salts at the interface, leading to substantial rubber encapsulation of the filler particles. As a consequence, the transfer of rubber from the bulk matrix to form an interlayer on the filler surface, reduces the reinforcing efficiency of the filler and lowers Young's modulus of the ternary phase composite.

Suppression of the reinforcing efficiency of glass beads encapsulated by MaR in the PP/MaR/G composite can also be demonstrated by consideration of Einstein [eq. (1)] and Kerner [eq. (2)] expressions for polymers filled with rigid spheres:

$$E_c/E_m = 1 + 2.5\phi_f \quad (1)$$

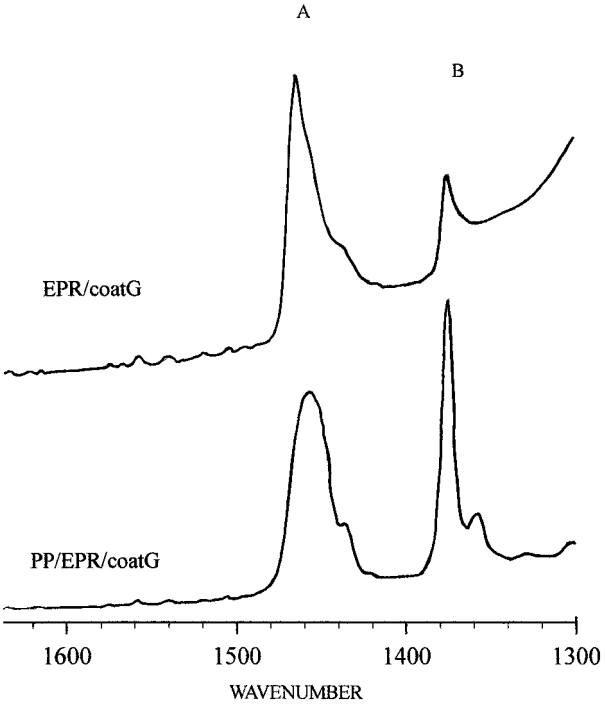

Figure 6 FTIR spectra of EPR/coatG and PP/EPR/coatG composites. (A) C—H stretch (CH_2 group); (B) C—H stretch (CH_3 group).

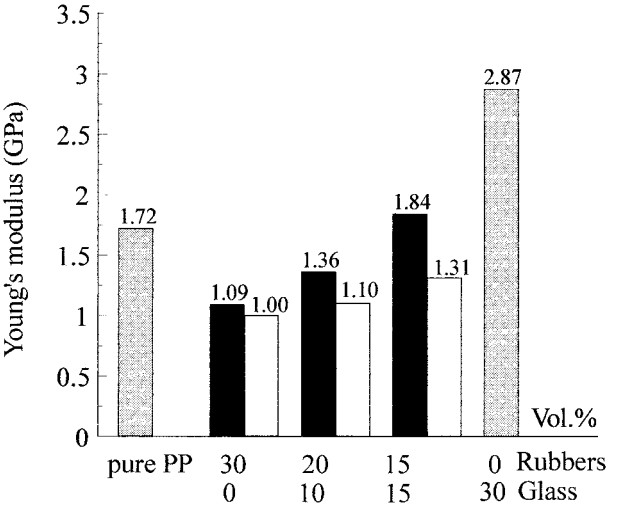

Figure 7 Young's modulus of PP, binary, and ternary phase PP composites. (■) Compositions containing EPR; (□) compositions containing MaR.

and

$$E_c/E_m = 1 + \{15(1 - \nu_m)/(8 - 10\phi_f)\}\{\phi_f/(1 - \phi_f)\} \quad (2)$$

E_c is modulus of the composite, E_m is modulus of the matrix polymer, ϕ_f is the volume fraction of filler, and ν_m the Poisson's ratio of the matrix. Experimental data measured from two-phase PP/EPR (70/15) and PP/MaR (70/15) compositions were taken as the matrix values for the PP/EPR/G (70/15/15) and PP/MaR/G (70/15/15) systems, respectively. Hence, E_m (PP/EPR) = 1.27 GPa and E_m (PP/MaR) = 1.09 GPa; 0.15 is the volume fraction of filler (ϕ_f), and 0.27 is Poisson's ratio (ν_m) for polypropylene.

Where filler is encapsulated by rubber, the experimental modulus is generally lower than that predicted. This is apparent in Table II, which shows that the measured modulus of the PP/MaR/G composite is lower than calculated values using either of these models, whereas the PP/EPR/G ternary blend with separate dispersion of EPR and G yielded a higher value than that predicted.

Tensile yield stress measurements for various PP composites are shown in Figure 8. Both rubber and uncoated glass beads caused a reduction in yield stress of the binary blends. In the PP/EPR/G composites, containing both rubber and filler, additivity effects were observed between the components, where measured yield stress was found to be a function of the total concentration of rubber and filler (Fig. 9). Similar behavior has been found in PP/EPDM/talc composites.[2] The PP/EPR/G formulation exhibited a higher yield stress than the corresponding PP/MaR/G composite, which can be attributed to inherent differences in the mechanical properties of the EPR elastomers.

Equation (3), proposed by Nielsen,[24] enables the strength of a filled polymer (σ_c) to be calculated from

Table II Experimental and Predicted Moduli Values for Ternary Phase PP Composites

Sample	Experimental Modulus (GPa)	Predicted Modulus (GPa)	
		Einstein	Kerner
PP/EPR/G	1.84	1.74	1.65
PP/MaR/G	1.31	1.49	1.42

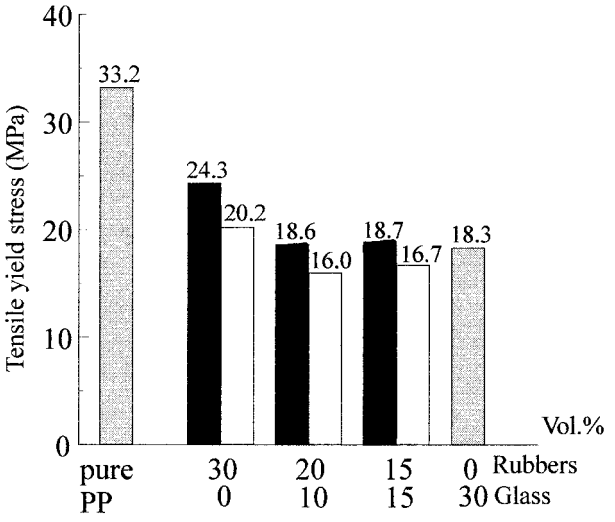

Figure 8 Tensile yield stress of PP, binary, and ternary phase PP composites. (■) Compositions containing EPR; (□) compositions containing MaR.

$$\sigma_c = \sigma_m(1 - \phi) \quad S \quad (3)$$

where σ_c and σ_m are the tensile strengths of the composite and matrix, respectively, and ϕ is the volume fraction of filler in the composite. A parameter S accounts for the weakness in the structure brought about by a discontinuity in stress transfer and the generation of a stress concentration at the filler–polymer interface. The maxi-

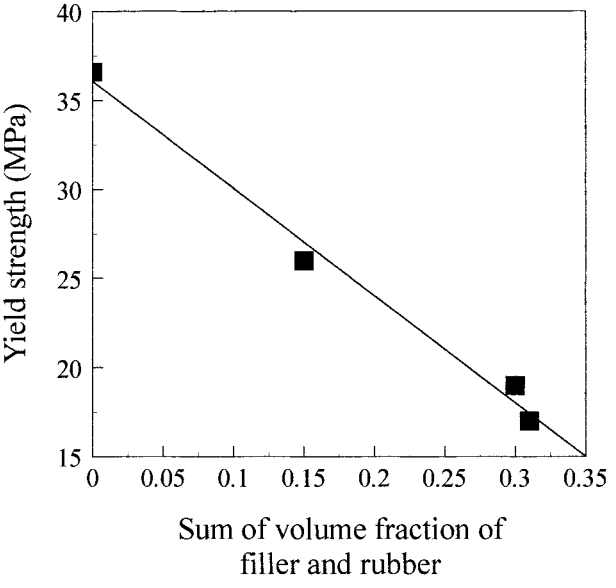

Figure 9 Influence of combined rubber and filler content on the tensile yield stress.

Table III Prediction of Tensile Strength in Ternary Phase PP Composites

Sample	σ_c (MPa)	σ_m (MPa)	S	a
PP/EPR/G	18.67	26.75	0.80	1.07
PP/MaR/G	16.73	19.49	1.00	0.50

S, from eq. (3); a, from eq. (4); σ_c and σ_m, tensile strengths of modulus and matrix, respectively.

mum value of S is unity, where stress concentrations are absent. The lower the value of S, the greater the stress concentration, or the poorer the adhesion.

Equation (4) was introduced by Nicolais and Nicodemo,[25] in which the strength of a filled composite can be expressed by

$$\sigma_c = \sigma_m(1 - a\phi^b) \quad (4)$$

where a and b are constants. The value of a is related to the stress concentration or the quality of adhesion between the matrix and filler, and b is dependent on the geometry of the filler. In spherical fillers uniformly distributed with no adhesion, a becomes 1.21. Where there is some adhesion, a becomes smaller than 1.21. The constant b is equal to 1 if the material fails by planar fracture and $\frac{2}{3}$ if it fails by random fracture.

From Table III, it is significant that the calculated value of S for the PP/MaR/G composite is 1, and the value of a is much smaller than 1.21, indicating that in this system there is good interfacial adhesion between the phases, leading to a continuity in stress transfer throughout the composite.

Table IV compares the impact properties of various PP composites. In binary blends, impact resistance of PP was significantly increased by the incorporation of EPR and, in particular MaR, rubbers. Comparing the effects of EPR and MaR on the failure energy of ternary phase composites, it can be seen that MaR was far more effective in raising overall impact resistance relative to PP, although the energy required for propagation of the crack in PP/MaR/G composites was lower than that in the PP/EPR/G formulations, yet crack initiation energy was higher. This reflects the strong interaction between MaR and glass beads, and is consistent with the cohesive and interfacial failure mechanisms shown earlier (Fig. 2) for ternary phase composites containing functionalized and unmodified EPR.

Table V shows the effects of introducing coatG on tensile and impact properties of ternary phase PP composites. Silane treatment on the glass has minimal effect on Young's modulus and tensile yield stress, although impact failure energy shows a marked increase. Because there is no apparent filler encapsulation in this system, the improvement in impact properties seen when coated glass is used could be due to its influence on composite morphological structure, including dispersion of fillers, rubber particle size, also the interparticle distance between phases. Interpretation of these mechanical and morphological data is complicated further by the possible influence of the rheology and viscosity of the composite. Work by Han and colleagues[26] showed that coupling agent may diffuse into the polymer, and by functioning as an internal plasticizer, cause a decrease in the viscosity of the matrix phase. Also, owing to a reduction in interfacial energy by the surface modifier, this may lead to reduced dispersed phase size and greater deformation of the rubber particles.[27]

Table IV Effect of Rubber Modifier on the Impact Properties of Binary and Ternary Phase PP Composites (at 23°C)

Composition PP/EPR/G (% by vol)	Initiation Energy (J)		Propagation Energy (J)		Failure Energy (J)	
	EPR	MaR	EPR	MaR	EPR	MaR
100/0/0	3.08		1.04		4.12	
70/30/0	5.33	6.41	1.99	2.58	7.32	8.99
70/20/10	2.59	4.11	1.24	0.79	3.83	4.90
70/15/15	3.11	5.59	1.47	1.15	4.57	6.74

Table V Influence of Glass Bead Surface Coating on the Mechanical Properties of Ternary Phase PP Composites (at 23°C)

		Tensile Properties				Impact Properties		
Sample	Composition (by vol)	Modulus (GPa)	Yield Stress (MPa)	Elongation at Yield (%)	Elongation at Break (%)	Initiation Energy (J)	Propagation Energy (J)	Failure Energy (J)
PP/EPR/G	100/0/0	1.72	33.24	5.77	146.88	3.08	1.04	4.12
PP/EPR/G	70/15/15	1.84	18.67	3.62	217.27	3.10	1.47	4.57
PP/EPR/coatG	70/15/15	1.73	18.80	3.83	254.64	4.10	1.93	6.03

CONCLUSIONS

The microstructure and mechanical properties of ternary phase PP composites containing EPR and G has been investigated. EPR and G were found to influence the structure and properties of PP in different ways. Incorporation of EPR into PP resulted in an improvement in impact strength, accompanied by a decrease in tensile strength and modulus. The opposite was found for composites containing glass beads. PP composites with balanced mechanical properties were achieved by physical blending of this polymer with both EPR and glass beads.

A study of the morphology of these compositions has shown that two kinds of structure can be formed, either a separate dispersion of the phases or encapsulation of the filler by rubber. A principal factor controlling formation of these structures was found to be the surface characteristics of the components. Modification of EPR by maleic grafting resulted in composites with rubber encapsulation of the filler, with FTIR revealing a reaction between these phases. Composites containing unmodified EPR, on the other hand, showed separate dispersion of the components. The former composites, exhibiting good adhesion at the rubber–filler interface, had noticeably higher impact strength, whereas the latter variant was characterized by higher tensile strength and modulus, accompanied by lower toughness. Improvement in impact strength of the composites was also achieved by introducing chemically treated glass beads.

REFERENCES

1. J. E. Stamhuis, *Polym. Compos.,* **5,** 202 (1984).
2. B. Pukanszky, J. Kolarik, and F. Lednicky, in *Polymer Composites,* B. Sedlacek, Ed., Walter de Gruyter, Berlin, 1986, p. 553.
3. B. Pukanszky, F. Tudos, J. Kolarik, and F. Lednicky, *Polym. Compos.,* **11,** 98 (1990).
4. J. Kolarik, F. Lednicky, J. Jancar, and B. Pukanszky, *Polym. Comm.,* **31,** 201 (1990).
5. J. Kolarik, and J. Jancar, *Polymer,* **33,** 4961 (1992).
6. J. Kolarik, and F. Lednicky, in *Polymer Composites,* B. Sedlacek, Ed., Walter de Gruyter, Berlin, 1986, p. 537.
7. J. Kolarik, B. Pukanszky, and F. Lednicky, *Compos. Polym.,* **2,** 271 (1990).
8. G. Marosi, G. Bertalan, I. Rusznak, P. Anna, and I. Molnar, in *Polymer Composites,* B. Sedlacek, Ed., Walter de Gruyter, Berlin, 1986, p. 457.
9. D. L. Faulkner, *J. Appl. Polym. Sci.,* **36,** 467 (1988).
10. W.-Y. Chiang, W. Yang, and B. Pukanszky, *Polym. Eng. Sci.,* **32,** 641 (1992).
11. R. Kosfeld, K. Schaefer, E. A. Kemmer, M. Hess, A. Theinsen, and T. H. Uhlenbroich, in *Controlled Interphases in Composite Materials,* H. Ishida, Ed., Elsevier Science Publishing Company, Amsterdam, 1990, p. 385.
12. K. C. Dao, and R. A. Hatem, *SPE ANTEC Tech. Papers,* **30,** 198 (1984).
13. H. Kitamura, *Proc. 4th Intl. Conf. Composite Mater.,* ICCM-IV, Tokyo, 1982, p. 1787.
14. P. G. Comitov, Z. G. Nicolova, I. S. Simeonov, K. V. Naidenova, and A. D. Siarova, *Eur. Polym. J.,* **20,** 405 (1984).
15. F. Danusso, and G. Gianotti, *Eur. Poly. J.,* **4,** 165 (1968).
16. A. McGregor, and L. E. Penins, *Plast. Polym.,* **38,** 192 (1970).
17. D. K. Owens, *J. Appl. Polym. Sci.,* **14,** 1725 (1970).
18. L. H. Lee, *J. Polym. Eng. Sci.,* **5,** 1103 (1967).
19. L. H. Lee, *Adhesion Science and Technology,* Vol. 9B, Plenum Press, New York, 1975, p. 647.
20. E. Sacher, *Symposium on Silylated Surfaces,* Gordon & Breach, London, 1983.

21. B. C. Trivedi, and B. M. Culbertson, *Maleic Anhydride,* Plenum Publishing Corporation, New York, 1982.
22. C. Scott, H. Ishida, and F. H. J. Maurer, *J. Mater. Sci.,* **22,** 3963 (1987).
23. E. P. Plueddemann, in *Interface in Polymer, Ceramic and Metal Matrix Composites,* H. Ishida, Ed., Elsevier Science Publishing Co., Amsterdam, 1988, p. 17.
24. L. E. Nielsen, *Mechanical Properties of Polymers and Composites,* Vol. 2, Marcel Dekker, New York, 1974.
25. L. Nicolais, and L. Nicodemo, *Polym. Eng. Sci.,* **13,** 469 (1973).
26. C. D. Han, T. Weghe, D. Shete, and J. R. Haw, *Polym. Eng. Sci.,* **21,** 196 (1981).
27. I. S. Miles, in *Multicomponent Polymer Systems,* I. S. Miles and S. Rostami, Eds., Longman Scientific & Technical, UK, 1992, Chap. 2.